ILASS–Europe 2017, 28th Conference on Liquid Atomization and Spray Systems, 6-8 September 2017, Valencia, Spain
http://dx.doi.org/10.4995/ILASS2017.2017.4697

Multi-scale Eulerian-Lagrangian simulation of a liquid jet in cross-flow under acoustic perturbations

Swann Thuillet*[1], Davide Zuzio[1], Olivier Rouzaud[1], Pierre Gajan[1]
[1]ONERA - The French Aerospace Lab
*Corresponding author: Swann.Thuillet@onera.fr

Abstract
The design of modern aeronautical propulsion systems is constantly optimized to reduce pollutant emissions while increasing fuel combustion efficiency. In order to get a proper mixing of fuel and air, Liquid Jets Injected in gaseous Crossflows (LJICF) are found in numerous injection devices. However, should combustion instabilities appear in the combustion chamber, the response of the liquid jet and its primary atomization is still largely unknown. Coupling between an unstable combustion and the fuel injection process has not been well understood and can result from multiple basic interactions.
The aim of this work is to predict by numerical simulation the effect of an acoustic perturbation of the shearing air flow on the primary breakup of a liquid jet. Being the DNS approach too expensive for the simulation of complex injector geometries, this paper proposes a numerical simulation of a LJICF based on a multiscale approach which can be easily integrated in industrial LES of combustion chambers. This approach results in coupling of two models: a two-fluid model, based on the Navier-Stokes equations for compressible fluids, able to capture the largest scales of the jet atomization and the breakup process of the liquid column; and a dispersed phase approach, used for describing the cloud of droplets created by the atomization of the liquid jet. The coupling of these two approaches is provided by an atomization and re-impact models, which ensure liquid transfer between the two-fluid model and the spray model. The resulting numerical method is meant to capture the main jet body characteristics, the generation of the liquid spray and the formation of a liquid film whenever the spray impacts a solid wall.
Three main features of the LJICF can be used to describe, in a steady state flow as well as under the effect of the acoustic perturbation, the jet atomization behavior: the jet trajectory, the jet breakup length and droplets size and distribution.
The steady state simulations provide good agreement with ONERA experiments conducted under the same conditions, characterized by a high Weber number (We>150). The multiscale computation gives the good trajectory of the liquid column and a good estimation of the column breakup location, for different liquid to air momentum flux ratios. The analysis of the droplet distribution in space is currently undergoing. A preliminary unsteady simulation was able to capture the oscillation of the jet trajectory, and the unsteady droplets generation responding to the acoustic perturbation.

Keywords
multiscale numerical simulation, liquid jet in gaseous crossflow, acoustic perturbation, Euler-Lagrange coupling

Introduction

The liquid jet in crossflow (LJICF) configuration covers several applications in engineering systems, such as combustion, chemical or even agriculture fields. Particularly in aircraft combustion chambers, systems where the fuel jet is injected normally into an air crossflow are commonly used. Compared with a free jet into a quiescent flow, this configuration enables a better mixing of fuel and air and fuel evaporation before delivery to the combustor. Therefore LJICF are found in numerous injection devices as the "Lean Preximed Prevaporizer" (LPP) device. However, this device operates on lean premixed combustion, a regime that easily leads to the apparition of combustion instabilities. Unstable combustion is the consequence of a thermo-acoustical coupling between instationary heat release from combustion and acoustic pressure oscillations in the combustion chamber. These instabilities lead to excessive engine vibration and possible irreversible damage of the propulsion system. Among the mechanisms that can be responsible for the variation of heat release from combustion, Apeloig [1] has shown the effect of : acoustic perturbations in the incoming airflow that creates fluctuations of the acoustic speed and pressure, state of the liquid phase injected in the combustion chamber (atomization, spray, filming), acoustic boundary conditions (including multiperfored liners [2]). The complete understanding of coupling mechanisms between unstable combustion and fuel injection process remains essential. The aim of our work is to perform a numerical simulation describing the behavior of a liquid jet in a subsonic gaseous crossflow under acoustic perturbation, thus improving the knowledge on the interaction between atomization and flow fluctuations.

Many studies have focused on steady-state LJICF. Mashayek et al. [2] gather the important parameters for the study of LJICF : the liquid and gaseous related physical parameters (density, viscosity, surface tension) and the parameters linked to the configuration, such as diameter of the jet and injector geometry. Pai et al. [3] identify four adimensional numbers for the jet behavior and atomization : the jet-to-crossflow momentum flux ratio q, the aerodynamic Weber number We_g, the liquid Reynolds number Re_l and the Ohnesorge number Oh_l. Wu et al. [4] studied experimentally the influence of these parameters on the behavior of the jet. They observed similarities

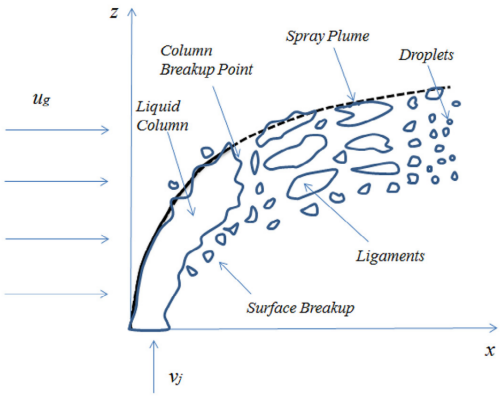

Figure 1. Liquid jet in crossflow configuration, from Broumand et al. [5]

between liquid jet primary breakup regimes and those reported by Hsiang and Faeth [6] for secondary breakup of droplets. Hence, they proposed a $q - We_g$ map to classify the jet primary breakup. These map shows different breakup regimes, such as the *column breakup*, the *multimode breakup* or *shear breakup*.
The liquid jet breakup generates different liquid structures : ligaments, droplets and blobs (Fig. 1). Experimentally, the jet breakup is usually characterized by four features [5] : liquid jet primary breakup regimes, liquid jet trajectory, liquid jet breakup length and spray characteristics. The first experimental studies [4] focused on large-scale features of the liquid jet breakup, such as trajectory of the jet and column breakup location. In a review paper, No [7] makes an inventory of the empirical correlations for trajectory of the jet. They showed a huge discrepancy between the different correlations obtained from experimental studies. Indeed, there are many factors that impacts the jet trajectory, and a restricted number of dimensionless numbers cannot characterize totally the jet trajectory over several regimes [7].

A few experimental studies on the effect of acoustic perturbations on LJICF have been performed. Carpentier et al. [8] investigated the comportment of a liquid jet in the presence of acoustic waves generated by a loudspeaker upstream a Kundt tube. The position of the jet orifice to the acoustic velocity nodes influences directly the jet destabilization, up to the jet atomization. Song et al. [9] studied the effect of a modulated crossflow on the spray formed by the liquid jet injection. They found out that an oscillating gaseous crossflow faintly changes the trajectory of the jet whereas it affects its atomization, resulting in smaller and more numerous droplets than in the steady case. They lately showed a periodic behavior regarding mean drop sizes and mean drop velocity. Unlike Song, Anderson et al. [10] observed a cyclical oscillation of the jet penetration when they increase the modulation level rate $\tau = \frac{\mathcal{V}'}{\bar{\mathcal{V}}}$. They came to the following conclusion : for a small τ only atomization process is impacted, when τ becomes stronger, the jet trajectory will also be modified by the modulated crossflow.

This study focuses on a high aerodynamic Weber number ($We_g > 110$), which is typical for *shear breakup*. In this type of primary breakup, the liquid jet is slightly deformed by the crossflow. Instabilities appears on the windward side of the liquid jet due to the strong shearing of the crossflow. These instabilities keep growing along the liquid jet and cause the breakup of the liquid column as a whole. Other instabilities are observed, creating ligaments then droplets stripped from the jet sides. These ligaments sizes have been widely studied by Sallam et al. [11], finding out that both the sizes of the ligaments and droplets increase with the distance from the orifice. Mazallon et al. [12] concluded that the length of the ligament increases progressively with the Ohnesorge number. This paper presents a multi-scale simulation of a LJICF in both stationary and perturbed gas flow up to the formation of the spray in the form of a dispersed phase.

Numerical Approaches
Phenomenological models have been developed to represent the mechanisms of primary breakup of the LJICF. Wang et al. [13] uses linear stability to describe the instability (especially Rayleigh-Taylor waves) of a round liquid jet in crossflow. They determined that three main terms contribute to the instability of the jet : jet velocity, surface tension and aerodynamic force.The analogy between jet atomization and "blobs" breaking up under Kelvin-Helmoltz instability enabled the development of two breakup models : the Taylor Analogy Breakup (TAB) [14] and the Wave breakup models [15]. These models can be easily integrated in Reynolds Averaged Navier-Stokes (RANS) computations.

Many numerical studies have been led with higher grid resolution, such as large eddy simulation (LES) [16]. This type of simulations represents large-scales features of the jet, but needs the development of sub-grid models to represent the drop generation process.
Direct numerical simulation (DNS) describes the whole atomization process from the larger scales to the smaller

ones. They are generally based on sharp interface computed by Level-Set method [17], Volume-of-Fluid [18], and derived methods such as Refined Level-Set [19] and Coupled Level-Set and Volume-of-Fluid [20]-[21]. These approaches require a large computational effort and can be combined with AMR method [22] to reduce the number of cells in the numerical domain or Euler-Lagrangian coupling (in a discrete element sense)[23].

The aim of this paper is to assess a new numerical approach based on a multi-scale methodology for the breakup of a liquid jet in cross-flow. The multi-scale methodology is described in the following section. While the two-fluid model captures the larger scale phenomena of the liquid jet breakup, the spray evolution is described by a well established dispersed phase model resolved in a Lagrangian framework. The Eulerian-Lagrangian coupling enables the simultaneous resolution of the two previous models. Being the DNS approach too expensive for the simulation of complex injector geometries, the multiscale approach provides a less expensive alternative that can be easily integrated in industrial LES of combustion chambers.
This multi-scale method is validated in the case of a liquid jet in steady gaseous crossflow. A preliminary unsteady simulation shows the effect of an oscillating crossflow on the jet behavior.

Numerical method
The multi-scale approach has been proposed by Blanchard [24] as a tool to be integrated in a LES framework. This approach has been already validated on the primary atomization of a sheared liquid sheet. This approach is based upon three numerical models :

- a two-fluid model based on finite volume discretization of conservation equation for both liquid and gas,
- a dispersed phase model with a Lagrangian solver which describes the motion of the droplets stripped from the jet,
- a sub-scale atomization model that detects zones where the droplets are produced. This model enables the exchanges between the two previous models.

The methodology has been implanted in to the ONERA legacy CEDRE code [25].

Two-fluid model
The two-fluid model (usually gas/liquid) considers two fluids simultaneously present in any point of the domain. The hypothesis of local mechanical equilibrium imposes that the two fluids have the same velocity and pressure within the given cell. The mass and momentum balance equation resolved by the model are :

$$\frac{\partial \tilde{\boldsymbol{\rho}}}{\partial t} + div\left(\tilde{\boldsymbol{\rho}} \otimes \boldsymbol{v}\right) = 0 \tag{1}$$

$$\frac{\partial \rho \boldsymbol{v}}{\partial t} + div\left(\rho \boldsymbol{v} \otimes \boldsymbol{v} + p\mathbf{I}\right) = div\left(\boldsymbol{\tau_v} + \boldsymbol{\tau_c}\right) + \rho \boldsymbol{g} + \boldsymbol{s}_p \tag{2}$$

with $\tilde{\boldsymbol{\rho}} = [\alpha_l \rho_l,\ \alpha_g \rho_g]^T = [\tilde{\rho_l},\ \tilde{\rho_g}]^T$ the fluid bulk densities, $\alpha_{l,g}$ the volume fractions of the liquid and the gas, $\rho_{l,g}$ the densities of the liquid and the gas, $\boldsymbol{\tau_c}$ and $\boldsymbol{\tau_v}$ respectively the capillary and viscous stress tensor, $\boldsymbol{g}$ the gravity acceleration and $\boldsymbol{s}_p$ the two-way coupling source term. The mixture density is $\rho = \alpha_l \rho_l + \alpha_g \rho_g$. As the configuration studied in this paper is iso-thermal, we do not consider the energy balance equation.

The numerical resolution of the system is done by finite volume scheme on unstructured 3D meshes. The time discretization is based on an explicit RK2 scheme. A second-order MUSCL scheme is used to achieve robust second order space accuracy, while a special attention has been paid to the multislope limitation procedure [26] in order to limit the diffusion of the interface.
Thermodynamic closure laws are considered for each phase : perfect gas and weakly compressible liquid [27].

Dispersed phase model
In a typical propulsion system, the number of droplets created from the fuel atomization can be huge, thus it is impossible to simulate each droplet individually. A statistical approach is chosen, based on the resolution of a Boltzmann equation [28] where a scalar function represents the average liquid droplets density. The resolution is based on a Lagrangian method, called particulate method. The dispersed phase model assumptions are :

- the droplets are rigid spheres,
- the spray is sufficiently diluted that the volume occupied by the droplet can be neglected,
- the evaporation, the secondary breakup and the collisions between droplets are not taken into account in the present simulations. Nevertheless, these features can be activated in the CEDRE code.

The concept of numerical particles is introduced, each particle being characterized by a numeric weight carrying the information of many physical droplets. These numerical particles obey transport equations. The spray is coupled to the carrier phase in a full two-way coupling. The numerical integration of this model is fully described in [24].

Atomization model

The atomization model couples the the two-fluid model and the dispersed phase model. This model must determine the location where the liquid is transferred from one model to another. The conservation of liquid mass and momentum is imposed between the two models.

The activation of the atomization model in a given cell is based on several criteria :

- the atomization should occur when the two-fluid solution is too diffuse,
- the model should not affect multifluid resolved liquid structures.

These criteria are rewritten with threshold values imposed by the user on the liquid volume fraction α_l and its gradient $\nabla\alpha_l$ calculated in the two-fluid model. The threshold on the volume fraction is set to $\alpha_l^{atom} = 0.1$, this value is a good compromise to trigger the atomisation where the liquid phase is diluted enough.The value of $\| \nabla\alpha_l \|^{atom}$ is directly linked to the interface thickness :

$$\delta_{int} \approx \frac{1}{\| \nabla\alpha_l \|^{atom}} \tag{3}$$

Thus, the threshold value must indicate a zone where the interface is diffuse enough, that is why we choose $\| \nabla\alpha_l \|^{atom} = C.\Delta x$ with $C = 0.5$ and Δx the local cell dimension.

Once the atomization is activated, the particles are injected in each cell Ω_i by respecting : the number of injected particles, the initial velocity of each droplet, the initial position randomly taken inside Ω_i, the physical properties of the droplets (same as the liquid), and diameter of the droplets. The diameter of the droplet is still a user-defined parameter at the present time. In this work, the diameter is chosen with the use of experimental correlations, thus representing the final diameter after primary and secondary atomization.

Results and discussion

Experimental set-up

Because of the few experimental studies that show the liquid jet in presence of an oscillationg crossflow, ONERA carried out an experimental investigation [29]. The purpose of this study is to understand the behavior of the spray generated from the breakup of a liquid jet in gaseous crossflow in the presence of combustion instabilities, and particularly the formation of liquid films when the droplets impact the duct walls.
The experimental configuration consists of a duct with rectangular cross-section where the liquid is injected by an circular orifice located on the bottom wall. Upstream, a loudspeaker delivers an imposed periodic acoustic perturbation. The figure 2 shows the experimental disposition, the highlighted rectangular area corresponds to the domain calculated by the numerical simulations. This domain has the following dimensions : $0.23\ m$ in length, $0.05\ m$ in width and $0.05\ m$ in height. A convergent section is placed just before the nozzle to reduce the duct height to $0.02\ m$, and thus stabilize the mean flow : the gas flow is considered as non-turbulent. The airflow velocities given in this paper refers to the velocity at the channel outlet. Several measurement methods provide us a significant database for the primary breakup of the liquid jet with a gaseous crossflow. The comparison between the numerical and experimental results on the same configuration allow to minimize the discrepancies due to the different geometrical and physical parameters (such as confinement or high-temperature effects).

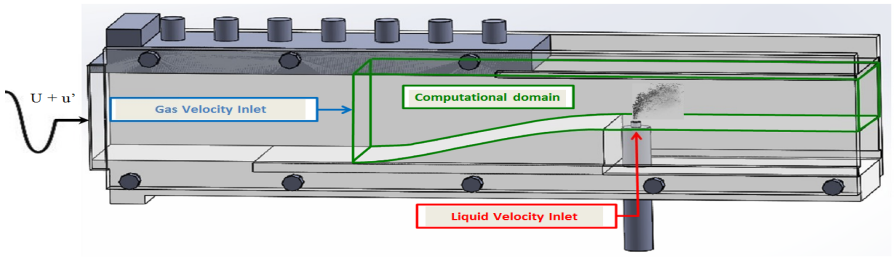

Figure 2. Experimental configuration set up at ONERA [29], the computational domain is highlighted in green

Steady flow simulations

First, we focus on a liquid jet injected in a steady gaseous crossflow. This configuration is chosen as representative as possible as a multipoint fuel injection device. The flow description is :

- the two fluids are respectively water for the liquid jet and air for the crossflow,
- the gaseous crossflow is laminar, the liquid jet is supposed laminar,
- the study is conducted at standard temperature and pressure (STP).

Table 1. Parameters of the simulation of the liquid jet in steady crossflow

Dimensional			
Jet diameter	d_j	2	mm
Air density	ρ_g	1.2	$kg.m^{-3}$
Water density	ρ_l	1000	$kg.m^{-3}$
Air viscosity	μ_g	$1.9\ 10^{-5}$	$Pa.s$
Water viscosity	μ_l	$1.\ 10^{-3}$	$Pa.s$
Air velocity	v_g	78	$m.s^{-1}$
Water velocity	v_l	$6.4 - 7.4 - 10.6$	$m.s^{-1}$
Surface tension	σ	0.072	$N.m^{-1}$
Non-dimensional			
Aerodynamic Weber number	$We_g = \frac{\rho_g d_j v_g^2}{\sigma}$		203
Jet-to-crossflow momentum flux ratio	$q = \frac{\rho_l v_l^2}{\rho_g v_g^2}$		$5.6 - 7.5 - 15.4$
Air Reynolds number	$Re_g = \frac{\rho_g d_j v_g}{\mu_g}$		9900
Ohnesorge number	$Oh_l = \frac{\mu_l}{\sqrt{\rho_l d_j \sigma}}$		$2.6\ 10^{-3}$
Jet-to-crossflow density ratio	$\Phi = \frac{\rho_l}{\rho_g}$		833

The computational domain is the same as the experimental setting presented in the previous subsection. The mesh consists of about 3.8 M elements, the most refined zone is along the jet inlet surface where the smallest cell size is $\Delta x = 80\ \mu m$. There are 30 cells in the section of the jet. The mesh becomes coarser downstream the injection point, where the dispersed phase model entirely describes the liquid phase. At the moment, no subgrid turbulence model has been activated as we are mainly interested in largest scales liquid/gas interactions. Turbulent effects will be taken in account in the future simulations. We choose an explicit time discretization, with a time step $\Delta t = 5.\ 10^{-8} s$. An effective parallelization on 480 processors enables to get a steady regime in approximately 10 hours CPU time.

The inlet gas velocity has a constant value of $v_g = 78\ m.s^{-1}$. The other physical parameters are summarized in table 2. As the liquid considered is water, the Ohnesorge number is $Oh_l = 2.64\ 10^{-3}$. As long as this number is smaller than 0.3, Sallam at al. [11] states that the viscous effects are small enough that the Ohnesorge number do not play any role to classify the jet primary breakup. The present Weber number is representative of the *shear breakup* regime.

Based on the correlations from Sallam's experimental observations [11], the droplet diameter has been fixed at $d_l = 100\ \mu m$. This diameter represents the droplets at the channel exit, after secondary breakup.

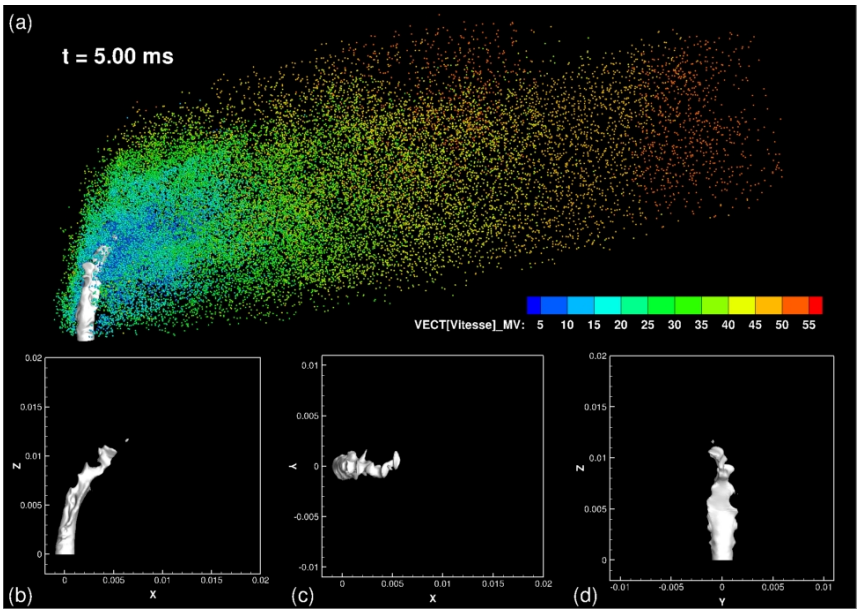

Figure 3. Simulation of the liquid jet in a gaseous steady crossflow

We firstly focus on the simulation with $q = 7.5$. The figure 3-(a) shows a snapshot of the simulated liquid jet in cross-flow, $5\ ms$ after the beginning of the liquid injection. The white shape represents the liquid core of the jet, depicted by the iso-contour $\alpha_l = 0.5$. This value of the liquid volume fraction α_l is chosen to define as precisely as possible the envelope which encloses most of the liquid. The particles are the Lagrangian droplets created by the atomization model.
The first step is to analyze the large scale features of the jet. We observe the development of the liquid jet bent by the crossflow. Waves propagate on the windward part of the jet, and these instabilities keep growing as they move along the jet up to provoke the breakup of the liquid column. A first estimation shows that the wavelength of these waves are slightly under the diameter jet (Fig. 3-(b)). Sallam et al. [11] give a correlation based on his experimental results, that leads to a wavelength of $\lambda_s = 0.3$. A protocol is actually developed to determine precisely the wavelength and the frequency of these waves.
As experimentally observed, the section of the jet is deformed and tends to a "kidney shape" (Fig. 3-(c)).
The analysis of the side view pictures of the jet enables to define jet trajectories for three differents value of q. These results have been compared to the experimental data [29] on the Figure 4.

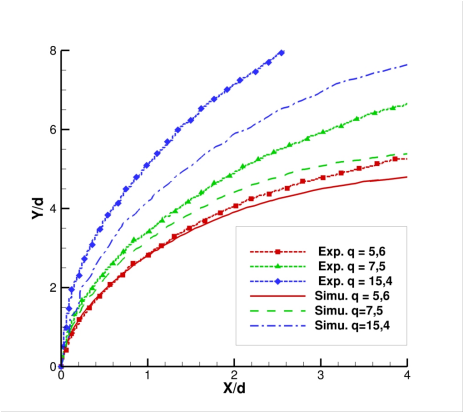

Figure 4. Effect of the q parameter on the jet trajectory

The numerical simulation results shows a further penetration of the liquid jet as the parameter q increases, in accordance with the experimental results [7]. Near the injection orifice ($\frac{x}{d_j} = 0.5$), the trajectories from numerical simulations are in a good agreement with the experimental observations. Beyond this point, the numerical curves tend to underestimate the jet trajectory, especially with increasing values of q. This may be explained by the liquid inlet conditions : laminar or turbulent profiles [16]. In our case the laminar profile seems to leads to a larger area exposed to the air flow, involving a stronger drag; this force increasing the jet bending.

With the side view of the liquid jet 3-(b), we can also estimate the mean column breakup location. The liquid jet breakup length corresponds to the streamwise distance reached by the liquid jet before its complete breakup. Even if the determination of the breakup length is not very accurate for several reasons [5], we will compare our results to experimental and numerical studies. The three numerical cases provides a constant normalized length $\frac{x_b}{d_j}$, around 5.2. Such a tendancy has also been observed in previous experimental studies [4]. Indeed, when the inlet liquid velocity increases, the penetration of the jet will tends to be more important while the breakup characteristic time is shorter. We compared our value of 5.2 with the data provided in the paper of Sallam et al. [11] and the theoretical value given by Wu et al. [4] of 8.6. Although our value appears far from Wu's value, the comparison with the experimental results from Sallam gives a good agreement, especially when the experimental conditions are closer to the considered configuration. Other numerical studies, such as Li and Soteriou [20] or Xiao et al. [16] also obtained similar values for the normalized breakup length.
Concerning the column breakup height y_b, the simulations give a proportionality $y_b \propto q^{0.47}$. Several authors [5] integrates other non-dimensional parameters in their correlation, such as Re_g or We_l. Here again, there is a large degree of discrepancies in literature for the prediction of the column breakup height, nevertheless the relation found in that study is in the range of the correlations given by Wu et al. [4]..

On the figure 3-(a), the particles are colored by their velocity magnitude. The initial velocity of the particles when they are generated is close to the liquid jet velocity magnitude. The particles velocities near the domain outlet are still mush smaller that the airflow velocity. Considering a characteristic length $l_0 = 0.1m$ equal to the distance between the jet orifice and the outlet to and v_g the gas flow velocity, the characteristic time of a particle and the Stokes number are :

$$t_0 = \frac{\rho_p d_p^2}{18\mu_g} = 0.029s, \qquad St = \frac{t_0 v_g}{l_0} = 21.8 \tag{4}$$

As the Stokes number is greater than 1, the particles are mostly driven by inertia and their relaxation to the air flow velocity is weak. The transit time of a particle in the domain is calculated with the length of the channel l_0 and a gas velocity $v_0 \approx 50\ m.s^{-1}$ slightly lower than the airflow velocity because of the jet wake :

$$t_p = \frac{l_0}{v_0} \approx 0.002s << t_0 \tag{5}$$

This explains that the particles velocity does not reach the airflow velocity before the channel exit.
A further analysis of the liquid jet and spray is currently in progress and will provide more details about the instabilities on the surface of the jet and the droplets distribution. These results will be compared to the data from ONERA experiments.

Unsteady flow simulation
The aim of this simulation is to show the capability of the multi-scale simulation to handle the propagation of an acoustic wave and its effect on the liquid jet behavior.

Table 2. Parameters of the simulation of the liquid jet in unsteady crossflow

Dimensional			
Air velocity	v_g	$39 \rightarrow 91$	$m.s^{-1}$
Water velocity	v_l	6.2	$m.s^{-1}$
Non-dimensional			
Aerodynamic Weber number	We_g	$51 \rightarrow 276$	
Jet-to-crossflow momentum flux ratio	q	$3.9 \rightarrow 21$	
Air Reynolds number	Re_g	$4900 \rightarrow 11500$	

The parameters of the simulation are given in the table 2. Starting from a steady state regime has been reached, then a periodic oscillation on the inlet acoustic velocity is imposed. The frequency of the oscillation is set to its experimental value $177Hz$. This frequency ensures the presence of a pressure node near the injection point, thus maximizing the acoustic velocity variations at this location. The modulation rate is $\tau = 40\ \%$.

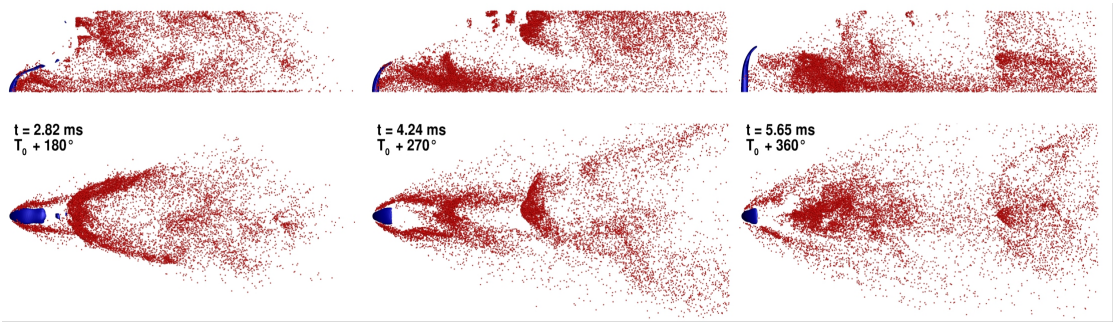

(a) (b) (c)

Figure 5. Simulation of the liquid jet in unsteady crossflow

Figure 5 shows snapshots of the jet at three different times after the beginning of the oscillation. The temporal phase is given in relation to the velocity oscillation imposed at the inlet. The blue shape is the liquid core of the jet, the Lagrangian particles are colored in red. Note that the atomization model has been activated at the beginning of the unsteady state, which can explain that the number of droplets is lower than the steady simulations presented in the previous part. The side views show that the liquid jet shape and penetration changes with the inlet velocity oscillation. Image processing of the numerical side views provides a frequency of the jet flapping around $177Hz$, consistent with the frequency of the upstream velocity oscillation.
A qualitative analysis of the pictures shows that the spray distribution depends on the time. For instance, a dense cloud of droplets reaches the upper wall at $t = T_0 + 180^\circ$ (Fig. 5-(a)) whereas the most dense region is located near the bottom wall at $t = T_0 + 270^\circ$ (Fig. 5-(b)). For all the three images, droplets are mainly clearly on the sides of the jet, as expected in such a flow regime. Besides, the unsteady spray distribution is qualitatively different from its steady counterpart (Fig. 3).
The simulation demonstrates the unsteady and heterogeneous characters of the spray distribution. When coupled with an evaporation model, it is expected to observe strong local variations of the mixture stoichiometry. Such a feature is consistent with the experimental observations of Apeloig [1].
This simulation is still in progress and additional analysis will provide more information about the liquid jet oscillation and the spray distribution. The numerical results will be compared to the experimental data from ONERA [29].

Conclusions

The simulation of a liquid jet in both steady and unsteady gaseous crossflow have been presented in this paper. The steady computation gives the good trajectory of the liquid column and a good estimation of the column breakup location, for different liquid to air momentum flux ratios. The unsteady simulations has shown the oscillation of the jet trajectory and the unsteady droplets generation responding to the acoustic perturbation. A quantitative study of the spray properties (distribution, velocities ...) is currently undergoing. The numerical data will be compared to the experiments conducted in ONERA.

The numerical approach is based on a multi-scale methodology. The results prove that the multi-scale methodology is able to capture the large scales of the LJICF and to reproduce the droplet generation from its breakup.

In a next step, evaporation processes will be taken into account [25]. Since there are still uncertainties on the data setting, the impact of the flow regime (laminar, turbulent ...) for both the liquid and gaseous phases will be also investigated.

One of the most important constraint to this method is the determination of the droplet radius. A predicting diameter model, such as an ELSA method, is considered to improve the proposal approach. This model will determine the local droplet size according to the actual atomization mechanisms. The model will be validated against the experimental observations.

References

[1] Apeloig, J., 2013, "Étude expérimentale du rôle de la phase liquide dans les phénomènes d'instabilités thermo-acoustiques agissant au sein de turbomachines diphasiques", Ph.D. thesis, ONERA.

[2] Mashayek, A., and Ashgriz, N. , 2011, "Atomization of a Liquid Jet in a Crossflow", Handbook of Atomization and Sprays, pp. 657-683.

[3] Pai, M., Pitsch, H., and Desjardins, O., 2009, "Detailed numerical simulations of primary atomization of liquid jets in crossflow", 47th AIAA Aerospace Sciences Meeting, p. 373.

[4] Wu, P. K., Kirkendall, K. A., Fuller, R. P., and Nejad, A. S., 1997, "Breakup processes of liquid jets in subsonic crossflows", Journal of Propulsion and Power, 13(1), pp. 64-73.

[5] Broumand, M., and Birouk, M., 2016, "Liquid jet in a subsonic gaseous crossflow: Recent progress and remaining challenges", Progress in Energy and Combustion Science, 57, 1-29.

[6] Hsiang, L. P., and Faeth, G. M., 1995," Drop deformation and breakup due to shock wave and steady disturbances", International Journal of Multiphase Flow, 21(4), pp. 545-560.

[7] No, S. Y., 2015, "A review on empirical correlations for jet/spray trajectory of liquid jet in uniform cross flow", International Journal of Spray and Combustion Dynamics, 7(4), pp. 283-313.

[8] Carpentier, J. B., Baillot, F., Blaisot, J. B., and Dumouchel, C., 2009, "Behavior of cylindrical liquid jets evolving in a transverse acoustic field", Physics of Fluids, 21(2).

[9] Song, J., Ramasubramanian, C., and Lee, J. G., 2014, "Response of Liquid Jet to Modulated Crossflow", Atomization and Sprays, 24(2).

[10] Anderson, T. J., Proscia, W., and Cohen, J. M., 2001, "Modulation of a liquid-fuel jet in an unsteady cross-flow", ASME Turbo Expo 2001: Power for Land, Sea, and Air, American Society of Mechanical Engineers.

[11] Sallam, K. A., Aalburg, C., and Faeth, G. M., 2004, "Breakup of round nonturbulent liquid jets in gaseous crossflow", AIAA journal, 42(12), pp. 2529-2540.

[12] Mazallon, J., Dai, Z., and Faeth, G. M., 1999, "Primary breakup of nonturbulent round liquid jets in gas crossflows", Atomization and Sprays, 9(3).

[13] Wang, S., Huang, Y., and Liu, Z. L., 2014, Theoretical analysis of surface waves on a round liquid jet in a gaseous crossflow, Atomization and Sprays, 24(1).

[14] O'Rourke, P. J., and Amsden, A. A., 1987, "The TAB method for numerical calculation of spray droplet breakup", Los Alamos National Lab., NM (USA).

[15] Reitz, R. D., and Bracco, F. V., 1982, "Mechanism of atomization of a liquid jet", The Physics of Fluids, 25(10).

[16] Xiao, F., Dianat, M., and McGuirk, J. J., 2013, "Large eddy simulation of liquid-jet primary breakup in air crossflow", AIAA journal, 51(12), pp. 2878-2893.

[17] Desjardins, O., and Pitsch, H., 2010, "Detailed numerical investigation of turbulent atomization of liquid jets", Atomization and Sprays, 20(4).

[18] Tomar, G., Fuster, D., Zaleski, S., and Popinet, S., 2010, "Multiscale simulations of primary atomization", Computers & Fluids, 39(10), pp. 1864-1874.

[19] Herrmann, M., 2008, "A balanced force refined level set grid method for two-phase flows on unstructured flow solver grids", Journal of Computational Physics, 227(4), pp. 2674-2706.

[20] Li, X., and Soteriou, M. C., 2014, "High-fidelity simulation of high density-ratio liquid jet atomization in crossflow with experimental validation", 26th Annual Conference on Liquid Atomization and Spray Systems, ILASS Americas (pp. 18-21).

[21] Ménard, T., Tanguy, S., and Berlemont, A., 2007, "Coupling level set/VOF/ghost fluid methods: Validation and application to 3D simulation of the primary break-up of a liquid jet", International Journal of Multiphase Flow, 33(5), pp. 510-524.

[22] Zuzio, D., and Estivalezes, J. L., 2011, "An efficient block parallel AMR method for two phase interfacial flow simulations", Computers & Fluids, 44(1), pp. 339-357.

[23] Herrmann, M., 2010, "A parallel Eulerian interface tracking/Lagrangian point particle multi-scale coupling procedure", Journal of Computational Physics, 229(3), pp. 745-759.

[24] Blanchard, G., 2014, "Modélisation et simulation multi-échelles de l'atomisation d'une nappe liquide cisaillée", Ph.D. thesis, ONERA.

[25] Refloch, A., Courbet, B., Murrone, A., Villedieu, P., Laurent, C., Gilbank, P., Troyes, J., Tessé, L., Chaineray, G., Dargaud, J., Quémerais, E., Vuillot, F., 2011, "CEDRE software", AerospaceLab, (2), p-1.

[26] Le Touze, C., Murrone, A., and Guillard, H., 2015, "Multislope MUSCL method for general unstructured meshes", Journal of Computational Physics, 284, pp. 389-418.

[27] Dutoya, D., and Matuszewski, L.,2011, "Thermodynamics in CEDRE", AerospaceLab, (2), p-1.

[28] Pai, M. G., and Subramaniam, S., 2009, A comprehensive probability density function formalism for multiphase flows, Journal of Fluid Mechanics, 628, p. 181.

[29] Desclaux A., 2016, "Étude de l'influence d'une excitation acoustique sur le comportement d'un jet liquide débouchant transversalement dans un écoulement d'air", Masters thesis, ONERA.